JOURNAL OF GEOPHYSICAL RESEARCH, VOL. 94, NO. B4, PAGES 3906-3922, APRIL 10, 1989

Brittle Frictional Mountain Building
1. Deformation and Mechanical Energy Budget

F. A. DAHLEN AND TERENCE D. BARR

Department of Geological and Geophysical Sciences, Princeton University, Princeton, New Jersey

An active fold-and-thrust belt is analogous to a wedge of soil or snow that forms in front of a moving bulldozer; such wedges exhibit a critical taper and a regional state of stress that is everywhere on the verge of Coulomb failure. The width of such a critically tapered fold-and-thrust belt does not depend on its brittle strength or frictional properties but rather on the accretionary influx rate of fresh material at its toe and on the rate of erosion; a steady state fold-and-thrust belt is one in which the accretionary influx is balanced by the erosive efflux. Rocks are accreted at the toe and then horizontally shortened as they are transported toward the rear; those that enter lower in the accreted section are more deeply buried before being uplifted by erosion. Mass balance and isotropy constrain the kinematics of this large-scale deformation, enabling us to infer the trajectories, residence times, and stress-strain histories of rocks incorporated into eroding fold-and-thrust belts. A typical rock resides in the steady state Taiwan wedge for 2–3 m.y. before it is uplifted and eroded; during its motion through the wedge, it experiences strain rates in the range 10^{-13} to 10^{-14} s^{-1}. The mechanical energy budget of brittle frictional mountain building is described by the equation $\dot{W}_B = \dot{W}_D + \dot{W}_S + \dot{W}_G$, where $\dot{W}_B$ is the rate of work performed on the base and front of the fold-and-thrust belt by the subducting plate, $\dot{W}_D$ is the rate at which energy is dissipated against friction on the decollement fault, $\dot{W}_S$ is the rate at which energy is dissipated by internal frictional processes within the deforming brittle wedge, and $\dot{W}_G$ is the rate of work performed against gravitational body forces in a reference frame attached to the overriding plate. The total mechanical power being supplied by the subducting Eurasian plate to the active fold-and-thrust belt in Taiwan is slightly over 3 GW. Approximately 60% of this work of steady state mountain building is being dissipated against friction on the decollement fault, and about another 25% is being dissipated against internal friction; this leaves only 15% or roughly half a gigawatt available to do useful work against gravity. In general, fold-and-thrust belts with moderate pore fluid pressures are dominated by work done against friction on the decollement fault; however, those with nearly lithostatic pore fluid pressures may be dominated by work done against gravity. Internal frictional dissipation is always less than basal frictional dissipation, as it is in Taiwan. An alternative and equivalent description of the mechanical energy balance of a steady state fold-and-thrust belt is provided by the equation $\dot{W}'_B = \dot{W}_D + \dot{W}_S + \dot{W}'_G$. In this version the quantity on the left, $\dot{W}'_B$, is the rate at which work is performed on the back of the wedge by the overriding plate and $\dot{W}'_G$ is the rate of work performed against gravity in a reference frame attached to the subducting plate. The latter quantity is always positive for any critically tapered fold-and-thrust belt whose decollement fault dips toward its rear, in contradiction to the central premise of the gravity spreading theory of fold-and-thrust tectonics.

INTRODUCTION

This is the first of two papers describing a simple model of the thermal structure and energy budget of foreland fold-and-thrust belts. The model is based on the premise that an actively deforming fold-and-thrust belt, like the wedge of soil that forms in front of a moving bulldozer, attains a critical taper in which the regional state of stress is on the verge of Coulomb failure everywhere [*Davis et al.*, 1983]. Critically tapered wedges with a planar decollement fault and negligible cohesion exhibit a perfectly triangular self-similar geometry, with the principal stress axes having the same orientation everywhere [*Dahlen*, 1984]. The magnitude of the critical taper is governed by the relative magnitudes of the basal sliding resistance and the Coulomb strength of the wedge material; increasing the basal traction increases the taper, whereas increasing the wedge strength decreases it. Erosion exerts a significant control on the mechanics of a fold-and-thrust belt, because an eroding wedge must continually deform throughout to maintain its critical taper. An active fold-and-thrust belt in unchanging tectonic and climatic conditions exhibits a steady state width when the influx of newly accreted material at the toe is balanced by the erosive efflux.

Here in paper 1 we develop a simple kinematic model of the regional deformation accompanying accretion and erosion and use it to analyze the mechanical energy balance of such a steady state fold-and-thrust belt. In paper 2 [*Barr and Dahlen*, this issue] we employ this kinematic model as the basis of a mechanically consistent thermal model; in addition to determining the steady state temperature distribution within a fold-and-thrust belt, the model determines the pressure-temperature-time trajectories of rocks that outcrop at the surface. We also combine our analysis of the mechanical energy budget with a similar analysis of the heat budget to obtain an estimate of the gross thermodynamic efficiency of brittle frictional mountain building. The principal focus of our modeling efforts is the active fold-and-thrust belt in Taiwan [*Suppe*, 1981, 1987; *Ernst*, 1982].

Paper number 88JB04333.
0148-0227/89/88JB-04333$05.00

STATE OF STRESS IN A CRITICALLY TAPERED WEDGE

We begin with a brief review of the critical Coulomb wedge model; for simplicity we restrict attention to the case of a

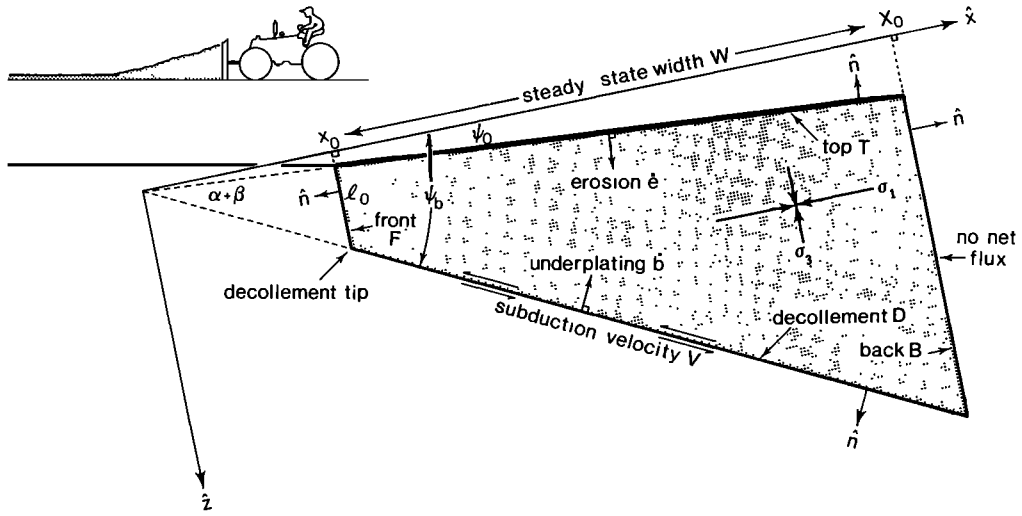

Fig. 1. Schematic cross section of a critically tapered steady state fold-and-thrust belt, indicating the principal axis coordinates x, z and other nomenclature employed in the derivation.

subaerial fold-and-thrust belt with negligible cohesion. Let $\mu = \tan\phi$ be the constant coefficient of internal friction of the wedge material, and let μ_b be the constant coefficient of sliding friction on the basal decollement. Let λ and λ_b be the constant ratios of pore fluid to lithostatic pressure [*Hubbert and Rubey*, 1959] in the wedge and on the base. The critical taper equation relating the constant surface slope α of an active fold-and-thrust belt to its constant basal dip β and its internal and basal strength parameters μ, μ_b, λ, and λ_b is then [*Dahlen*, 1984]

$$\alpha + \beta = \psi_b - \psi_0 \tag{1}$$

where

$$\frac{\tan 2\psi_0}{\csc\phi \sec 2\psi_0 - 1} = \frac{\tan\alpha}{1-\lambda} \tag{2}$$

$$\frac{\tan 2\psi_b}{\csc\phi \sec 2\psi_b - 1} = \frac{\mu_b(1-\lambda_b)}{1-\lambda} \tag{3}$$

The angles ψ_0 and ψ_b are the constant acute angles between the axis of principal compressive stress and the top and bottom of the wedge, so that equation (1) expresses an elementary relationship between two internal angles and the opposite external angle of a triangle. The width of a fold-and-thrust belt governed by friction and brittle failure is unrestricted by mechanical strength considerations, provided that the taper $\alpha + \beta$ is given by equation (1).

It is convenient in deriving the kinematic model below to use coordinates x, z that are aligned along the principal axes; in that case, ψ_0 and ψ_b are also the angles between the x axis and the top and bottom of the wedge, as shown in Figure 1. Let σ_1 and σ_3 denote the greatest and least principal solid stresses, and let P_f denote the pore fluid pressure, with the convention that compressive stresses are regarded as negative. The effective principal stresses $\bar{\sigma}_1 = \sigma_1 + P_f$ and $\bar{\sigma}_3 = \sigma_3 + P_f$ are given in terms of x and z within the wedge by [*Dahlen*, 1984]

$$\bar{\sigma}_1 = -(1-\lambda)\rho g \cos\alpha\,(z\cos\psi_0 - x\sin\psi_0)\left[\frac{1+\sin\phi}{1-\sin\phi\cos 2\psi_0}\right] \tag{4a}$$

$$\bar{\sigma}_3 = -(1-\lambda)\rho g \cos\alpha\,(z\cos\psi_0 - x\sin\psi_0)\left[\frac{1-\sin\phi}{1-\sin\phi\cos 2\psi_0}\right] \tag{4b}$$

where ρ is the constant rock density. The ratio $\bar{\sigma}_1/\bar{\sigma}_3$ is a constant depending only on the internal friction, namely,

$$\frac{\bar{\sigma}_1}{\bar{\sigma}_3} = \frac{1+\sin\phi}{1-\sin\phi} \tag{5}$$

and this is one version of the Coulomb failure criterion [*Jaeger and Cook*, 1969]. The variation of pore fluid pressure P_f within the wedge is given by

$$P_f = \lambda\rho g \cos\alpha\,(z\cos\psi_0 - x\sin\psi_0) \tag{6}$$

whereas the mean solid pressure $P = -\frac{1}{2}(\sigma_1 + \sigma_3)$ is given by

$$P = \rho g \cos\alpha\,(z\cos\psi_0 - x\sin\psi_0)\left[\frac{1-\lambda\sin\phi\cos 2\psi_0}{1-\sin\phi\cos 2\psi_0}\right] \tag{7}$$

The constant fluid/solid pressure ratio

$$\frac{P_f}{P} = \frac{\lambda(1-\sin\phi\cos 2\psi_0)}{1-\lambda\sin\phi\cos 2\psi_0} \tag{8}$$

approaches unity only in the limit of lithostatic pore pressure $\lambda = 1$; more generally, it is in the range $0 \le P_f/P \le \lambda$, and this has important consequences for brittle foreland metamorphism.

Shear failure within the Coulomb wedge material occurs on conjugate thrust faults oriented at angles $\pm\frac{1}{2}(90° - \phi)$ with respect to the σ_1 or x axis. The failure stress $|\tau|$ on these thrusts at the point where they step up into the wedge is given by

$$|\tau| = \rho g x \sin\alpha \, (\tan\psi_b \cos\psi_0 - \sin\psi_0) \left[\frac{\cos\phi}{\sin 2\psi_0} \right] \quad (9)$$

whereas the frictional resistance τ_b on the basal decollement at the same point is

$$\tau_b = \rho g x \sin\alpha \, (\tan\psi_b \cos\psi_0 - \sin\psi_0) \left[\frac{\sin 2\psi_b}{\sin 2\psi_0} \right] \quad (10)$$

The quantity $\tau_b/|\tau| = (\sin 2\psi_b)/(\cos\phi)$ is a constant measure of the ratio of decollement fault strength to overlying wedge strength, which must be between zero and one for every compressive fold-and-thrust belt.

KINEMATICS OF LARGE-SCALE DEFORMATION

The state of stress (4) in a critical Coulomb wedge is determined by a purely static analysis of the balance of forces. We now supplement that analysis with a simple kinematic description of the steady state deformation of an actively accreting and eroding, critically tapered fold-and-thrust belt; the model is basically that developed by *Dahlen and Suppe* [1988], with some refinements. Let the coordinates of the outcrop point of the deformation front be x_0, $x_0 \tan\psi_0$, and let those of the tip of the decollement fault be x_0, $x_0 \tan\psi_b$ as shown in Figure 1. The quantity

$$l_0 = x_0 \, (\tan\psi_b - \tan\psi_0) \quad (11)$$

is then the thickness (measured in the z direction) of the undeformed sedimentary sequence being accreted at the toe. We adopt a frame of reference fixed to the overriding plate and denote the steady Eulerian velocity of rocks in this frame by

$$\mathbf{u} = u\hat{\mathbf{x}} + v\hat{\mathbf{z}} \quad (12)$$

The cross-sectional accretionary influx $\dot{A}$ is related to the velocity at the deformation front by

$$\dot{A} = \int_{x_0 \tan\psi_0}^{x_0 \tan\psi_b} u \, dz \quad (13)$$

We regard $\dot{A}$ as known; in practice, it is estimated by multiplying the plate convergence rate times the thickness of the accreted sediments.

Assumptions

At every point within the wedge we make two assumptions, which suffice to determine $\mathbf{u}$. The first is that compaction of the wedge material subsequent to accretion is negligible, in which case

$$\frac{\partial u}{\partial x} + \frac{\partial v}{\partial z} = 0 \quad (14)$$

This assumption of incompressibility is consistent with the assumed constancy of the density ρ in the critical taper model, and it should be a good approximation whenever the entering sediments are thick and reasonably well lithified. Drilling data indicate that the mean density of the coastal plain rocks entering the Taiwan wedge is about 2400 kg/m^3, whereas the maximum density of rocks in the easternmost interior of the fold-and-thrust belt is about 2700 kg/m^3 [*Davis et al.*, 1983]. The volumetric strain due to compaction and metamorphism is thus about 10–15%, which is negligible in comparison with the model shear strains of 500–1000% [*Dahlen and Suppe*, 1988].

The second assumption we make is that on a regional scale, the wedge material is isotropic; this is a common assumption made in engineering applications of the theory of plasticity [*Hill*, 1950]. In an isotropic material the principal strain rates $\dot{\varepsilon}_1 = \partial u/\partial x$ and $\dot{\varepsilon}_3 = \partial v/\partial z$ must be everywhere aligned with the principal stresses σ_1 and σ_3. In our x, z coordinate system this condition takes the simple form

$$\frac{\partial v}{\partial x} + \frac{\partial u}{\partial z} = 0 \quad (15)$$

The likelihood of stratigraphically controlled planes of weakness and the predominance of forward verging thrust faults make isotropy a more questionable assumption than incompressibility, but we show below that it actually provides a far less significant constraint on the solution, because of the thin-skinned nature of fold-and-thrust belts.

Boundary Conditions and Flux Balance

The uplift rate on the upper surface of a steady state wedge must be everywhere equal to the erosion rate. If the local rate at which material leaves the wedge due to erosion is denoted by $\dot{e}$, then this boundary condition can be written in the form

$$u \sin\psi_0 - v \cos\psi_0 = \dot{e} \quad \text{on} \quad z = x \tan\psi_0 \quad (16)$$

In addition to accretion $\dot{A}$ at the toe, material may be underplated to a wedge beneath its base by the imbrication and assimilation of duplexes wherever the decollement fault steps down [*Silver et al.*, 1985]. If $\dot{b}$ is the local rate at which at which this underplated material enters the wedge, then the corresponding boundary condition on the decollement fault is, by analogy with (16),

$$u \sin\psi_b - v \cos\psi_b = \dot{b} \quad \text{on} \quad z = x \tan\psi_b \quad (17)$$

By conservation of mass, the total flux entering and leaving an arbitrary section of wedge between x_0 and some point x must balance. This condition can be written in the form

$$\dot{A} + \sec\psi_b \int_{x_0}^{x} \dot{b} \, dx = \sec\psi_0 \int_{x_0}^{x} \dot{e} \, dx + \int_{x \tan\psi_0}^{x \tan\psi_b} u \, dz \quad (18)$$

where the terms on the left represent the influx due to accretion at the toe and underplating and those on the right represent the efflux due to erosion and horizontal transport. Let X_0 be the point where the flux of material in the x direction vanishes, i.e.,

$$\int_{X_0 \tan \psi_0}^{X_0 \tan \psi_b} u \, dz = 0 \tag{19}$$

The quantity $W = X_0 - x_0$ given by

$$\dot{A} + \sec \psi_b \int_{x_0}^{x_0 + W} \dot{b} \, dx = \sec \psi_0 \int_{x_0}^{x_0 + W} \dot{e} \, dx \tag{20}$$

is then the width of a steady state wedge, whose total influx is completely balanced by erosion. To find the velocity $\mathbf{u}$, it is unnecessary to specify the location of either the front or the back boundary of a steady state wedge precisely, since the boundary conditions there involve only the net flux. For simplicity, however, we consider the wedge to be bounded by the planar surfaces $x = x_0$ and $x = X_0$, as shown in Figure 1.

Determination of the Velocity

The general solution to equations (14)–(15) is of the form

$$\mathbf{u} = \mathbf{u}_p + C \mathbf{u}_h \tag{21}$$

where $\mathbf{u}_h$ is a homogeneous solution corresponding to the case where there is no erosion or underplating and $\mathbf{u}_p$ is a particular solution satisfying the boundary conditions (16)–(17). It is easily verified that an appropriate homogeneous solution is

$$u_h = x^{-1} (1 - z^2/x^2)^{-1} \tag{22a}$$

$$v_h = z x^{-2} (1 - z^2/x^2)^{-1} \tag{22b}$$

which corresponds to a simple channel flow whose streamlines and trajectories are straight lines diverging from the origin.

The particular solution $\mathbf{u}_p$ depends on the detailed specification of $\dot{e}$ and $\dot{b}$. For simplicity, we consider only the idealized case of uniform underplating

$$\dot{b} = \dot{b}_0 \tag{23}$$

where $\dot{b}_0$ is a constant. We likewise consider an idealized erosion law of the form

$$\dot{e} = \dot{e}_0 + E h \tag{24}$$

where $\dot{e}_0$ and E are constants, and

$$h = x \sin \alpha \sec \psi_0 \tag{25}$$

is the height of the eroding point above the wedge vertex. This is a composite of two limiting cases: $\dot{e} = \dot{e}_0$, which corresponds to uniform erosion over the entire mountain belt, and $\dot{e} = E h$, which accounts for the possibility of increased erosion at higher elevations. Such a linear elevation-dependent law is motivated by the linear relation between erosion rate and relief that has been observed in a number of denudation studies in various climatic and vegetative conditions [*Ruxton and McDougall*, 1957; *Ahnert*, 1970]. Relief, however, is not synonymous with elevation, and that makes the justification for preferring linear to uniform erosion less than compelling. In any case, the difference between the solutions $\mathbf{u}$ obtained in the two cases is moderate, as we show below. The composite particular solution satisfying equations (23) and (24) is

$$u_p = U_0 + B (x - z \sin 2\psi_b) \tag{26a}$$

$$v_p = V_0 + B (x \sin 2\psi_b - z) \tag{26b}$$

where

$$U_0 = \frac{-\dot{e}_0 \sec \psi_0 + \dot{b}_0 \sec \psi_b}{\tan \psi_b - \tan \psi_0} \tag{27a}$$

$$V_0 = \frac{-\dot{e}_0 \sec \psi_0 \tan \psi_b + \dot{b}_0 \sec \psi_b \tan \psi_0}{\tan \psi_b - \tan \psi_0} \tag{27b}$$

$$B = \frac{-E \sin \alpha}{\sin 2\psi_b - \sin 2\psi_0} \tag{27c}$$

Collecting these results, we find that the Eulerian velocity field $\mathbf{u}$ within the model steady state wedge is given by

$$u = U_0 + B (x - z \sin 2\psi_b) + C x^{-1} (1 - z^2/x^2)^{-1} \tag{28a}$$

$$v = V_0 + B (x \sin 2\psi_b - z) + C z x^{-2} (1 - z^2/x^2)^{-1} \tag{28b}$$

The unknown constant C is obtained from the flux balance condition (20), with the result

$$C = \frac{2\dot{A} + 2x_0 (\dot{e}_0 \sec \psi_0 - \dot{b}_0 \sec \psi_b) + E x_0^2 \sin \alpha \sec^2 \psi_0}{\log \left[\dfrac{(1 + \tan \psi_b) (1 - \tan \psi_0)}{(1 - \tan \psi_b) (1 + \tan \psi_0)} \right]} \tag{29}$$

The steady state width W is related to the flux rate constants and wedge geometry by the quadratic equation

$$\tfrac{1}{2} E \sin \alpha \sec^2 \psi_0 (W^2 + 2x_0 W) + (\dot{e}_0 \sec \psi_0 - \dot{b}_0 \sec \psi_b) W - \dot{A} = 0 \tag{30}$$

In the case of uniform erosion, $E = 0$, this reduces to

$$W = \frac{\dot{A}}{\dot{e}_0 \sec \psi_0 - \dot{b}_0 \sec \psi_b} \tag{31}$$

whereas if $\dot{e}_0 = \dot{b}_0 = 0$, it reduces to

$$W = \left[\frac{2\dot{A}}{E \sin \alpha \sec^2 \psi_0} + x_0^2 \right]^{\frac{1}{2}} - x_0 \tag{32}$$

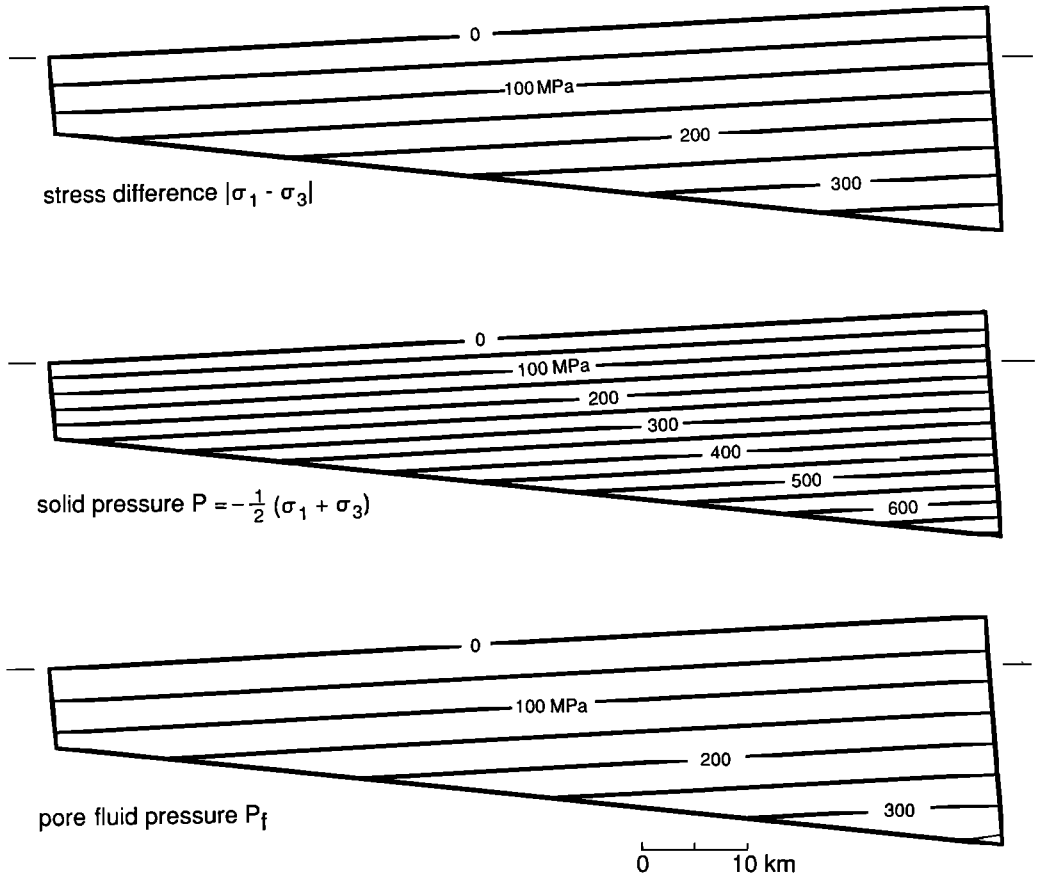

Fig. 2. Theoretical cross sections of the Taiwan fold-and-thrust belt (no vertical exaggeration) showing the variation with depth of the principal stress difference $|\sigma_1 - \sigma_3|$, the mean solid pressure P, and the pore fluid pressure P_f. The constant slope of the topographic surface is $\alpha = 3°$, and the dip of the basal decollement fault is $\beta = 6°$. The steady state width of the fold-and-thrust belt, measured along the top, is $W = 90$ km, and the thickness of the undeformed sedimentary sequence just being accreted along the oblique left margin is $l_0 = 7$ km. The coefficients of basal and internal friction are $\mu_b = 0.5$ and $\mu = 0.7$.

Strain and Slip Rates and Particle Trajectories

The local principal strain rates $\dot{\varepsilon}_1 = \partial u/\partial x$ and $\dot{\varepsilon}_3 = \partial v/\partial z$ are given by

$$\dot{\varepsilon}_1 = -\dot{\varepsilon}_3 = B - Cx^{-2}(1 + z^2/x^2)(1 - z^2/x^2)^{-2} \quad (33)$$

and the downdip velocity $V = u\cos\psi_b + v\sin\psi_b$ at the decollement tip x_0, $x_0\tan\psi_b$ is

$$V = U_0\cos\psi_b + V_0\sin\psi_b + Bx_0\cos\psi_b(1 - \tan^2\psi_b) + Cx_0^{-1}\sec\psi_b(1 - \tan^2\psi_b)^{-1} \quad (34)$$

We regard the downgoing plate beneath the decollement as rigid and take V to be its constant subduction velocity. The slip rate $\Delta u = V - u\cos\psi_b - v\sin\psi_b$ is then zero at the tip of the decollement fault where rocks are just being accreted, and it varies along the fault as

$$\Delta u = C(xx_0)^{-1}(x - x_0)\sec\psi_b(1 - \tan^2\psi_b)^{-1} - B(x - x_0)\cos\psi_b(1 - \tan^2\psi_b) \quad (35)$$

Rock trajectories $x(t)$, $z(t)$ within the wedge can be found by numerically solving the set of first-order coupled equations

$$dx/dt = u(x, z); \quad dz/dt = v(x, z) \quad (36)$$

The initial conditions for rocks entering the toe at $t = 0$ are $x(0) = x_0$, $z(0) = z_0$, where $x_0\tan\psi_0 \le z_0 \le x_0\tan\psi_b$.

APPLICATION TO TAIWAN

The island of Taiwan is the site of an ongoing collision between the Luzon island arc on the Philippine Sea plate and the stable continental margin of China on the Eurasian plate. The divergence between the strike of the arc and the continental margin results in a southward propagating collision that began about 4 m.y. ago in the north and is occurring now at the southern tip of the island [*Suppe*, 1981; *Chi et al.*, 1981]. Farther to the south, the oceanic crust of the South China Sea is subducting beneath the Luzon arc along the Manila Trench, and a recent study of the three-dimensional seismic velocity structure of the region shows evidence for the subduction of Eurasian continental crust everywhere beneath Taiwan [*Roecker et al.*,

1987]. Once the accretionary wedge between the trench and the arc has risen above sea level to become the Western Foothills, Hsuehshan Range, and Central Mountains of Taiwan, it can no longer grow unobstructedly because of erosion. Between 100 and 300 km north of the southern tip of the island, the mountains exhibit a remarkably uniform surface slope and width; this morphology suggests strongly that the fold-and-thrust belt in this region has attained a dynamic steady state in which the accretionary influx is balanced by the erosive efflux [*Suppe*, 1981].

Taiwan is an ideal natural laboratory for studying brittle frictional mountain building, because its structure and other properties have been well determined through extensive deep drilling, seismic reflection profiling, and detailed surface mapping conducted for petroleum exploration. The steady state region of the fold-and-thrust belt is characterized by a regional dip of the decollement fault $\beta = 6°$, a regional surface slope $\alpha = 3°$, a pore fluid/lithostatic pressure ratio $\lambda = \lambda_b = 0.7$, and a mean rock density $\rho = 2500$ kg/m^3 [*Davis et al.*, 1983; *Dahlen et al.*, 1984]. These observed values are consistent with the critical taper equations (1)–(3) for many combinations of μ_b and μ, since increasing μ_b increases the taper whereas increasing μ decreases it. The level of friction has a significant effect on the thermal structure of an actively accreting and eroding wedge, and we show in paper 2 that a coefficient of basal friction $\mu_b = 0.5$ provides the best fit to observed surface heat flow and cooling history data from Taiwan. The corresponding value of the coefficient of internal friction consistent with the observed geometry and pore fluid pressure is $\mu = 0.7$, in which case $\phi = 35°$, $\psi_0 = 4°$, and $\psi_b = 13°$. We adopt these values in all the analysis that follows, unless stated otherwise.

The width of the region of steady state topography in Taiwan is

$$W = 90 \text{ km} \tag{37}$$

and the average thickness of the sedimentary sequence accreted at the toe is [*Suppe*, 1981]

$$l_0 = 7 \text{ km} \tag{38}$$

The distance from the deformation front to the submerged wedge vertex used as the origin of coordinates is found from equation (11) to be

$$x_0 = 45 \text{ km} \tag{39}$$

Figure 2 depicts the theoretical cross section of a critically tapered wedge having these parameters, with superimposed contours of the principal stress difference $|\sigma_1 - \sigma_3| = |\bar{\sigma}_1 - \bar{\sigma}_3|$, the mean solid pressure $P = -\frac{1}{2}(\sigma_1 + \sigma_3)$ and the pore fluid pressure P_f. All the contours are parallel to the upper surface of the wedge; the constant fluid/solid pressure ratio is $P_f/P = 0.5$.

The accretionary influx rate at the toe is estimated by *Suppe* [1981] to be about

$$\dot{A} = 500 \text{ km}^2\text{/m.y.} \tag{40}$$

The corresponding steady state uniform erosion rate found from equation (31), assuming there is no underplating ($\dot{b}_0 = 0$), is

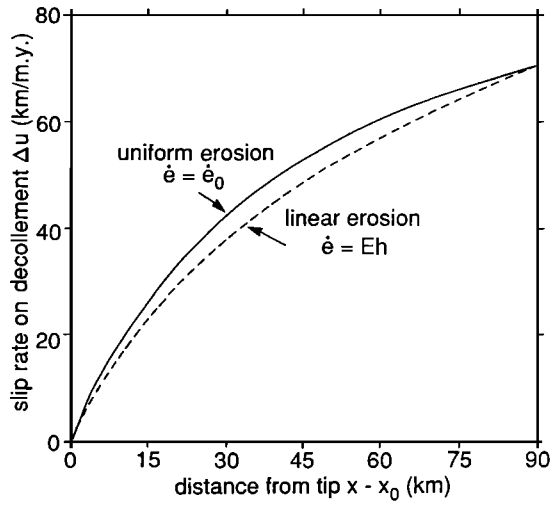

Fig. 3. Comparison of the theoretical slip rate Δu on the basal decollement fault under the Taiwan fold-and-thrust belt, for the case of uniform erosion $e = \dot{e}_0$ and linear elevation-dependent erosion $\dot{e} = Eh$. The slip rate increases rapidly to about 40 km/m.y. in the front 30 km and then more slowly to the full subduction velocity $V = 70$ km/m.y. at the rear. Distance along the abscissa is measured in the x direction; the actual distance from the tip along the fault is $(x - x_0)\sec\psi_b$.

$$\dot{e}_0 = 5.5 \text{ km/m.y.} \tag{41}$$

If, on the other hand, the erosion law is $\dot{e} = Eh$, we find from equation (32) that

$$E = 1.2 \text{ (m.y.)}^{-1} \tag{42}$$

In the latter case the local erosion rate varies linearly from 2.8 km/m.y. at the deformation front to 8.3 km/m.y. at the crest of the fold-and-thrust belt. The observed average rate of erosion in Taiwan, determined from both suspended and dissolved stream loads [*Li*, 1976] and radiocarbon dating of uplifted Holocene reefs and marine terraces [*Peng et al.*, 1977], is in the range 5–6 km/m.y. This good agreement between measured and inferred average erosion rates provides additional evidence for the steady state nature of the deformation [*Suppe*, 1981]. The available hydrologic and geomorphologic data are not, however, adequate to determine whether the uniform or linear erosion law is more appropriate.

The subduction velocity of the downgoing Eurasian plate is found from equation (34) to be

$$V = 70 \text{ km/m.y.} \tag{43}$$

if either $\dot{e} = \dot{e}_0 = 5.5$ km/m.y. or $\dot{e} = Eh$ with $E = 1.2$ (m.y.)$^{-1}$. This inferred value is in good agreement with the observed northwest-southeast convergence rate between the Eurasian and Philippine Sea plates in the vicinity of Taiwan [*Seno*, 1977; *Ranken et al.*, 1984], as expected. The inferred slip rate on the decollement fault is shown in Figure 3; it is evident that the results do not depend strongly on the form of the erosion law. The rate of increase of Δu in the front half of the wedge is greater in the case $\dot{e} = \dot{e}_0$ since material must be moving more rapidly to replace the greater loss due to erosion; conversely, it is greater in the back half of the wedge in the case $\dot{e} = Eh$ for

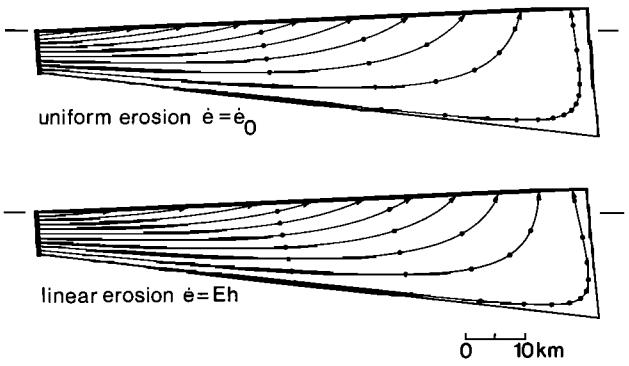

Fig. 4. Comparison of the theoretical trajectories of rocks in the Taiwan fold-and-thrust belt, for the case of uniform erosion $\dot{e} = \dot{e}_0$ and linear elevation-dependent erosion $\dot{e} = Eh$. The dots depicting rock positions every 1 m.y. show that horizontal transport is slightly faster in the front half of the wedge, and slightly slower in the back half, if the erosion is uniform. Rocks that enter the wedge just above the tip of the decollement fault are buried the deepest and have the longest residence time; they outcrop after 12–15 m.y. in the very rear of the fold-and-thrust belt. The residence time of most rocks is, however, only 2 to 3 m.y.

the same reason. The slip rate at the back of the wedge, 90 km from the tip, is equal to the subduction velocity, indicating that the overlying material there is moving with the Philippine Sea plate.

The theoretical trajectories of rocks moving through the steady state Taiwan fold-and-thrust belt are illustrated in Figure 4; the dots depict the motion of rocks along these streamlines at 1-m.y. intervals. The relatively minor difference between the results for the two erosion laws is again evident; to a very good approximation, the rocks in either case move across the wedge in columns that shorten uniformly in the σ_1 or x direction and stretch uniformly in the σ_3 or z direction, as in the pure shear kinematic model of *Dahlen and Suppe* [1988]. Rocks are transported almost halfway across the fold-and-thrust belt in 1 m.y. and about two thirds of the way across in 3 m.y. The uppermost 2–3 km of entering section are uplifted and eroded in less than 1 m.y., whereas rocks lower in the section are buried and transported farther into the fold-and-thrust belt before they are uplifted. Qualitatively, the trajectories resemble those in the viscous corner flow models of *Cowan and Silling* [1978], *Cloos* [1982], and *Wang and Shi* [1984]. Note, however, that in the present model, no rigid backstop has been imposed to drive the flow upward at the back of the fold-and-thrust belt; rather, the uplift is a natural consequence of the surface erosion. Furthermore, the present model is not based on an unrealistic viscous rheology; instead it is intended to represent the purely brittle regional-scale deformation of a critically tapered fold-and-thrust belt in the upper crust. As we show below, the kinematics in a thin-skinned wedge is effectively controlled completely by mass balance: if incompressible rocks enter at the toe and only leave by being eroded more slowly off the top, then they must move through the wedge as shown in Figure 4. As noted above, the analysis is not significantly affected by our specific choice for the geometry of the back boundary; all the rocks in the vicinity of $x_0 + W$ can be regarded as fully accreted.

Contours of the inferred strain rate $|\dot{\varepsilon}_1| = \dot{\varepsilon}_3$ within the Taiwan fold-and-thrust belt are shown in Figure 5. Although this differentiated quantity is particularly sensitive to the form of the erosion law, the difference between the two results is still slight; the strain rate is 2–2.5 $(\text{m.y.})^{-1}$ or 6×10^{-14} to 8×10^{-14} s^{-1} near the toe of the fold-and-thrust belt, and it decreases to about 0.3 $(\text{m.y.})^{-1}$ or 1×10^{-14} s^{-1} at the back. Similar values have been inferred from analyses of naturally deformed rock samples taken from orogenic belts by *Pfiffner and Ramsay* [1982]; a direct comparison with such studies may not be too meaningful, however, since the model estimates are measures of the total strain rate due to large-scale as well as small-scale processes, and much of the regional-scale shortening in fold-and-thrust belts is due to the imbrication of major thrust faults.

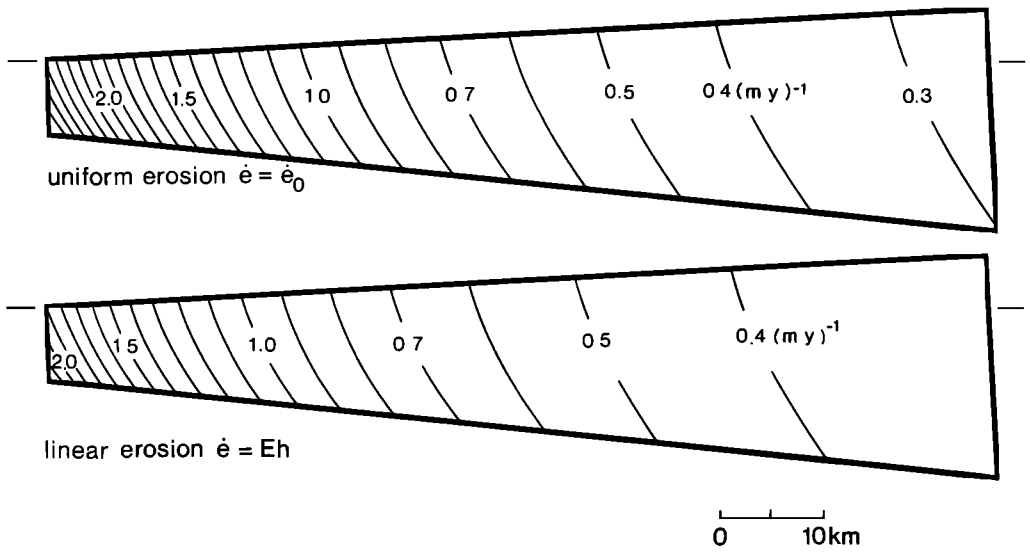

Fig. 5. Comparison of the theoretical instantaneous strain rate $|\dot{\varepsilon}_1| = \dot{\varepsilon}_3$ within the Taiwan fold-and-thrust belt, for the case of uniform erosion $\dot{e} = \dot{e}_0$ and linear elevation-dependent erosion $\dot{e} = Eh$. The highest strain rates, exceeding 1 $(\text{m.y.})^{-1}$ or 3×10^{-14} s^{-1}, are concentrated in the front one third of the wedge.

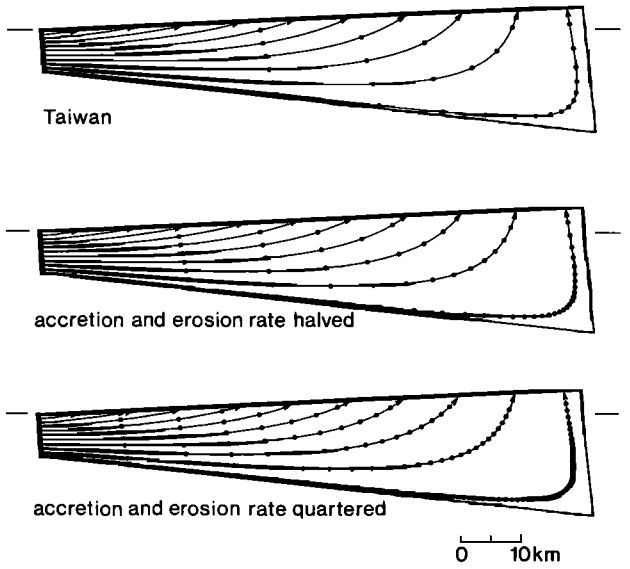

Fig. 6. If the accretion rate $\dot{A}$ and the uniform erosion rate $\dot{e}_0$ are both decreased by the same factor, then the width W of the steady state wedge and the streamlines within it are unchanged, but the motion of rocks along the streamlines is faster by the same factor.

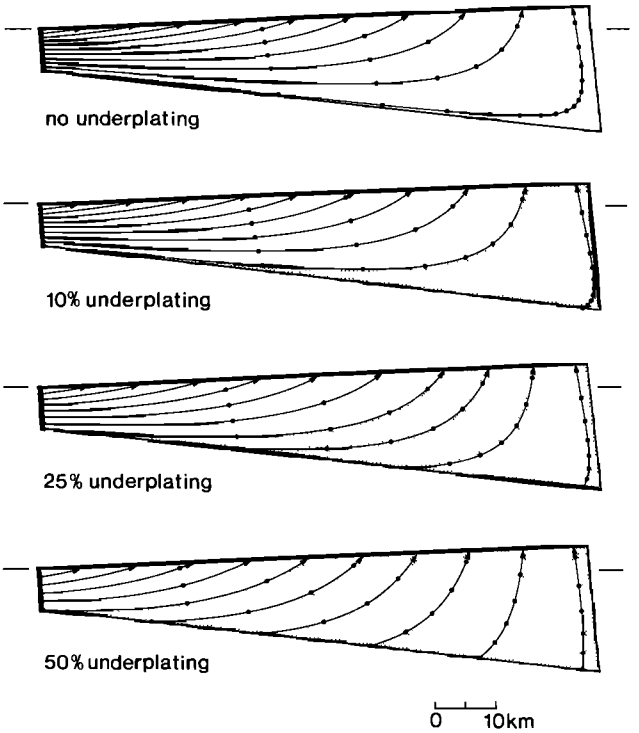

Fig. 8. Theoretical trajectories of rocks in the steady state fold-and-thrust belt of Taiwan, for the case of uniform erosion $\dot{e}_0 = 5.5$ km/m.y. and various amounts of underplating $\dot{b}_0$. Stippling denotes rocks that were underplated beneath the basal decollement fault. If 50% of the influx is due to underplating, then the bulk of the wedge consists of underplated rocks; all the rocks accreted at the toe are in that case uplifted and eroded within 1–2 m.y. in the front half of the wedge.

The erosion rate in Taiwan is one of the highest in the world due to a combination of high rainfall and susceptible lithology [*Stallard*, 1988]. Figure 6 shows the theoretical trajectories through two hypothetical fold-and-thrust belts having the same geometry as Taiwan, but with accretion and uniform erosion rates that are reduced by factors of one half and one quarter. The streamlines are identical but the velocity is everywhere slower by the same factor; such reduced material flux rates have a significant effect on the thermal structure, as we show in paper 2. If the erosion rate is lower, but the accretion rate remains the same, then the rate of horizontal transport is instead everywhere faster; this is illustrated in Figure 7, where we plot the theoretical outcrop position of an entering rock versus its residence time, again assuming uniform erosion. The faster transport is offset by the greater width of a more slowly eroding fold-and-thrust belt, so that the residence time of a rock with a given entering depth is essentially independent of the erosion rate.

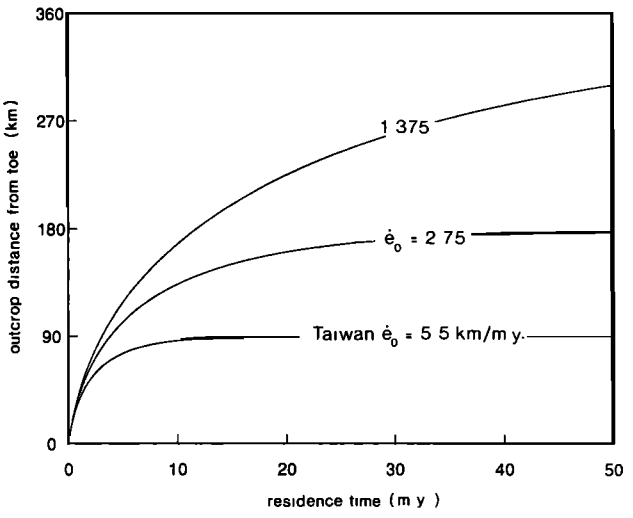

Fig. 7. Theoretical outcrop position versus residence time of rocks moving through the Taiwan wedge, for various values of the uniform erosion rate $\dot{e}_0$, assuming $\dot{A} = 500$ km/m.y. The transport is most rapid near the toe where the distance traveled varies like $t^{1/2}$. The steady state widths for the three cases shown are $W = 90$ km, $W = 180$ km and $W = 360$ km; in the latter case, the erosion and uplift rate is one quarter that in Taiwan, and horizontal velocities are still appreciable after 50 m.y.

Figure 8 illustrates the kinematic consequences of underplating in a hypothetical fold-and-thrust belt with the same geometry and uniform erosion rate as Taiwan. The total influx rate $\dot{A} + \dot{b}_0 W \sec\psi_b$ has been fixed at 500 km^2/m.y. to retain the same steady state width, and the percent underplating is the flux ratio $R = (\dot{b}_0 W \sec\psi_b)/(\dot{A} + \dot{b}_0 W \sec\psi_b)$. To a first approximation, the underplated rocks outcrop in the back R percent of the fold-and-thrust belt and comprise about $R^{1/2}$ percent of its total volume if there is R percent underplating. It is difficult to rule out 10–25% underplating in Taiwan, because of uncertainties in the plate convergence velocity, incoming sediment thickness, and average erosion rate; more than 25% underplating, however, probably can be ruled out.

Mechanical Energy Budget

The static equilibrium equation within the wedge is

$$\nabla \cdot \boldsymbol{\sigma} + \rho \mathbf{g} = 0 \tag{44}$$

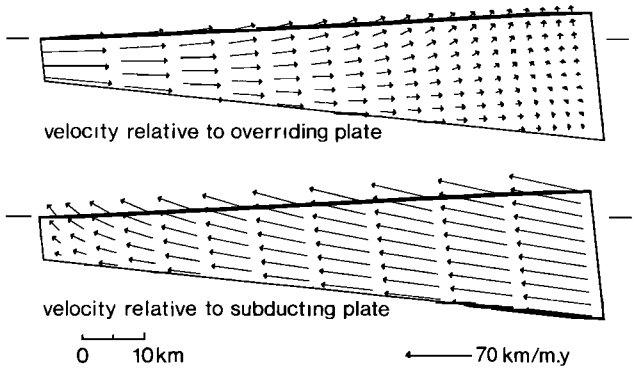

Fig. 9. (Top) Theoretical steady state velocity $\mathbf{u}$ of rocks within the steady state Taiwan wedge, assuming no underplating and uniform erosion $\dot{e}_0 = 5.5$ km/m.y. This velocity field relative to the overriding plate is the one that is integrated to find the rock trajectories in Figures 4, 6, 7, and 8. (Bottom) The corresponding velocity $\mathbf{u}'$ relative to the subducting plate is dominated throughout most of the wedge by the rigid motion $-V\cos\psi_b\,\hat{\mathbf{x}} - V\sin\psi_b\,\hat{\mathbf{z}}$ up the decollement fault. The flux of material through the toe is nearly zero in this frame of reference, and velocities on the back are nearly constant, and equal to the velocity of the bulldozer.

where $\boldsymbol{\sigma}$ is the stress tensor and $\mathbf{g}$ is the gravitational acceleration. This equation is valid either in a frame of reference attached to the overriding plate or in one attached to the subducting plate, and an analysis of the mechanical energy budget can be conducted in either of these two frames. By continuity, the rigid subducting plate must have a component of velocity b_0 normal to the decollement fault if there is underplating. The velocity field within the wedge relative to the subducting plate is thus given in general by $\mathbf{u}' = \mathbf{u} - \mathbf{U}$, where

$$\mathbf{U} = (V\cos\psi_b + \dot{b}_0\sin\psi_b)\,\hat{\mathbf{x}} + (V\sin\psi_b - \dot{b}_0\cos\psi_b)\,\hat{\mathbf{z}} \tag{45}$$

The velocity fields $\mathbf{u}$ and $\mathbf{u}'$ relative to the overriding and subducting plates are compared for the case of no underplating and uniform erosion in Figure 9.

To determine the balance of mechanical energy in the frame of reference of the overriding plate, we take the dot product of equation (44) with $\mathbf{u}$ and integrate over the volume M formed by extending the wedge cross section a unit distance along strike. Let T, F, B, and D denote the top, front, back, and decollement boundary surfaces, as shown in Figure 1. After an integration by parts we obtain

$$\int_{T+F+B+D} \hat{\mathbf{n}}\cdot\boldsymbol{\sigma}\cdot\mathbf{u}\,dA - \int_M \boldsymbol{\sigma}:\dot{\boldsymbol{\varepsilon}}\,dV + \int_M \rho\mathbf{g}\cdot\mathbf{u}\,dV = 0 \tag{46}$$

where $\dot{\boldsymbol{\varepsilon}} = \frac{1}{2}[\nabla\mathbf{u} + (\nabla\mathbf{u})^T]$ is the strain rate tensor and $\hat{\mathbf{n}}$ is the unit outward normal. The quantity $\boldsymbol{\sigma}:\dot{\boldsymbol{\varepsilon}}$ is the local rate at which energy is dissipated against internal friction within the wedge; it is given in terms of the principal stresses and strain rates by $\boldsymbol{\sigma}:\dot{\boldsymbol{\varepsilon}} = \sigma_1\dot{\varepsilon}_1 + \sigma_3\dot{\varepsilon}_3$. The brittle deformation within the model wedge is accommodated by means of slip along a continuously distributed network of conjugate thrust faults oriented at angles $\frac{1}{2}(90° - \phi)$ with respect to the axis of principal stress, and the quantity $\sigma_1\dot{\varepsilon}_1 + \sigma_3\dot{\varepsilon}_3$ can be regarded as the rate of frictional dissipation on these faults.

The integral over the top surface T vanishes since $\hat{\mathbf{n}}\cdot\boldsymbol{\sigma} = 0$ there. The integral over the decollement surface D can be written without any approximation in the form

$$\int_D \hat{\mathbf{n}}\cdot\boldsymbol{\sigma}\cdot\mathbf{u}\,dA = [V + \mu_b^{-1}(1-\lambda_b)^{-1}\dot{b}_0]\int_D \tau_b\,dA - \int_D \tau_b\,\Delta u\,dA \tag{47}$$

where τ_b is the basal shear traction and Δu is the rate of slip. On the back surface B the quantity $\hat{\mathbf{n}}\cdot\boldsymbol{\sigma}\cdot\mathbf{u}$ reduces to $\sigma_1 u$, and on the front surface F it reduces to $-\sigma_1 u$. Furthermore, u is very nearly zero on B, whereas $u \simeq V\cos\psi_b + \dot{b}_0\sin\psi_b$ on F; we therefore have, to a very good approximation,

$$\int_{F+B} \hat{\mathbf{n}}\cdot\boldsymbol{\sigma}\cdot\mathbf{u}\,dA = -[V\cos\psi_b + \dot{b}_0\sin\psi_b]\int_F \sigma_1\,dA \tag{48}$$

Upon resolving the remaining quantities in equation (46) into principal coordinates, we obtain the final result

$$\dot{W}_B = \dot{W}_D + \dot{W}_S + \dot{W}_G \tag{49}$$

where

$$\begin{aligned}\dot{W}_B &= [V + \mu_b^{-1}(1-\lambda_b)^{-1}\dot{b}_0]\int_D \tau_b\,dA \\ &\quad - [V\cos\psi_b + \dot{b}_0\sin\psi_b]\int_F \sigma_1\,dA \\ &= [V + \mu_b^{-1}(1-\lambda_b)^{-1}\dot{b}_0]\sec\psi_b\int_{x_0}^{X_0}\tau_b\,dx \\ &\quad - [V\cos\psi_b + \dot{b}_0\sin\psi_b]\int_{x_0\tan\psi_0}^{x_0\tan\psi_b}\sigma_1\,dz\end{aligned} \tag{50a}$$

$$\dot{W}_D = \int_D \tau_b\,\Delta u\,dA = \sec\psi_b\int_{x_0}^{X_0}\tau_b\,\Delta u\,dx \tag{50b}$$

$$\dot{W}_S = \int_M \boldsymbol{\sigma}:\dot{\boldsymbol{\varepsilon}}\,dV = \int_{x_0}^{X_0}dx\int_{x\tan\psi_0}^{x\tan\psi_b}(\sigma_1\dot{\varepsilon}_1 + \sigma_3\dot{\varepsilon}_3)\,dz \tag{50c}$$

$$\begin{aligned}\dot{W}_G &= -\int_M \rho\mathbf{g}\cdot\mathbf{u}\,dV \\ &= \rho g\int_{x_0}^{X_0}dx\int_{x\tan\psi_0}^{x\tan\psi_b}[u\sin(\alpha+\psi_0) - v\cos(\alpha+\psi_0)]\,dz\end{aligned} \tag{50d}$$

Equation (49) expresses the fundamental balance of mechanical energy in the reference frame of the overriding plate. The quantity $\dot{W}_B$ on the left is the rate at which the subducting plate performs work on the base and front of the critically tapered steady state fold-and-thrust belt, and the three terms on the right represent the three ways in which this work is either dissipated or expended. The quantity $\dot{W}_D$ is the rate of work dissipated against sliding friction on the decollement fault, whereas $\dot{W}_S$ is

the rate of work dissipated against internal friction within the wedge. In both cases the dissipated energy is primarily manifested as heat, although $\dot{W}_S$ also incorporates any surface energy required to create fresh fractures within the brittle wedge [*Rice*, 1980; *Wong*, 1982]. The final quantity $\dot{W}_G$ is the rate of work done in uplifting rocks against gravitational body forces in the reference frame of the overriding plate. All the rates of work are measured per unit length along the strike of the fold-and-thrust belt.

To determine the balance of energy in the frame of reference of the subducting plate, we take the dot product of equation (44) with $\mathbf{u}'$ rather than $\mathbf{u}$ and integrate over M to obtain

$$\int_{T+F+B+D} \hat{\mathbf{n}}\cdot\boldsymbol{\sigma}\cdot\mathbf{u}'\,dA - \int_M \boldsymbol{\sigma}:\dot{\boldsymbol{\varepsilon}}\,dV + \int_M \rho\mathbf{g}\cdot\mathbf{u}'\,dV = 0 \quad (51)$$

The strain rate $\dot{\boldsymbol{\varepsilon}}$ in equation (51) is the same as that in equation (46) since $\nabla\mathbf{u}' = \nabla(\mathbf{u} + \mathbf{U}) = \nabla\mathbf{u}$. In this case the integral over the decollement surface D reduces to

$$\int_D \hat{\mathbf{n}}\cdot\boldsymbol{\sigma}\cdot\mathbf{u}'\,dA = -\int_D \tau_b\,\Delta u\,dA \quad (52)$$

Since $u' \simeq 0$ on F whereas $u' \simeq -V\cos\psi_b - \dot{b}_0\sin\psi_b$ on B, we have, to a very good approximation,

$$\int_{F+B} \hat{\mathbf{n}}\cdot\boldsymbol{\sigma}\cdot\mathbf{u}'\,dA = -[\,V\cos\psi_b + \dot{b}_0\sin\psi_b\,]\int_B \sigma_1\,dA \quad (53)$$

The energy balance equation in the reference frame of the subducting plate thus takes the form

$$\dot{W}'_B = \dot{W}_D + \dot{W}_S + \dot{W}'_G \quad (54)$$

where

$$\dot{W}'_B = -[\,V\cos\psi_b + \dot{b}\sin\psi_b\,]\int_B \sigma_1\,dA$$

$$= -[\,V\cos\psi_b + \dot{b}_0\sin\psi_b\,]\int_{x_0\tan\psi_0}^{x_0\tan\psi_b} \sigma_1\,dz \quad (55a)$$

$$\dot{W}'_G = -\int_M \rho\mathbf{g}\cdot\mathbf{u}'\,dV$$

$$= \rho g\int_0^{x_0} dx \int_{x\tan\psi_0}^{x\tan\psi_b} [\,(u - V\cos\psi_b - \dot{b}_0\sin\psi_b)\sin(\alpha+\psi_0)$$

$$-(v - V\sin\psi_b + \dot{b}_0\cos\psi_b)\cos(\alpha+\psi_0)\,]\,dz \quad (55b)$$

In this case the quantity $\dot{W}'_B$ on the left is the rate of work performed on the back of the fold-and-thrust belt by the overriding plate, and $\dot{W}'_G$ is the rate of work done against gravity in the reference frame of the subducting plate.

The two versions of the mechanical energy balance are illustrated and compared in the the cartoon in Figure 10. The quantity $\dot{W}'_B$ is analogous to the rate of work performed on a moving wedge by a bulldozer, whereas $\dot{W}_B$ is analogous to the rate of work required to pull a Mylar sheet beneath a stationary buttressed wedge in a laboratory sandbox experiment [*Davis et al.*, 1983]. Physically, it is the sinking of the subducting plate rather than the bulldozing action of the overriding plate that is the ultimate source of the mechanical energy supplied to a fold-and-thrust belt. For this reason, it is preferable to use the first version of the energy balance in calculating the gross thermodynamic efficiency of brittle frictional mountain building, as we do in paper 2. A straightforward application of Gauss's theorem shows that the two forms of the energy balance are consistent, since $\dot{W}'_B = \dot{W}_B + \Delta\dot{W}$ and $\dot{W}'_G = \dot{W}_G + \Delta\dot{W}$, where

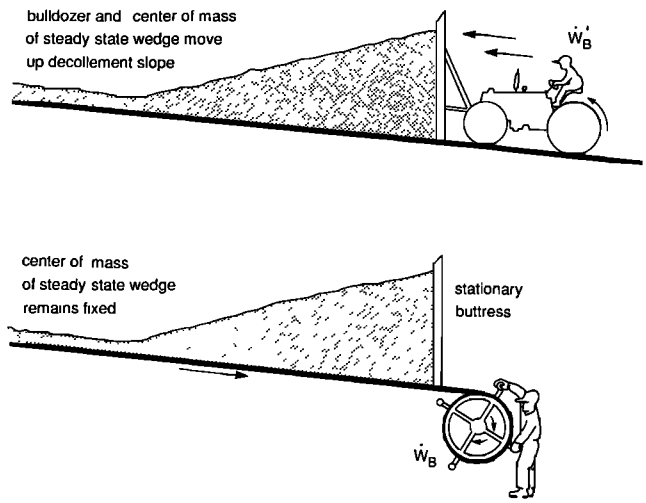

Fig. 10. Both the mechanical work needed to deform and emplace a fold-and-thrust belt and the portion of that work used to uplift rocks against gravity are frame-dependent. From the viewpoint of an observer situated on the subducting plate, the rate of work $\dot{W}_B$ performed on the back of the fold-and-thrust belt is analogous to the work performed by a moving bulldozer. From the viewpoint of an observer on the overriding plate, the rate of work $\dot{W}'_B$ performed on the base and front of the fold-and-thrust belt is analogous to the work required to pull a Mylar sheet beneath a buttressed wedge in a laboratory sandbox experiment. The two rates of work are related by $\dot{W}'_B = \dot{W}_B + \Delta\dot{W}$, where $\Delta\dot{W}$ is the rate at which work must be done to move the center of mass up the decollement slope in the reference frame of the subducting plate.

$$\Delta\dot{W} = \int_M \rho\mathbf{g}\cdot\mathbf{U}\,dV = \tfrac{1}{2}\rho g W(W + 2x_0)(\tan\psi_b - \tan\psi_0)$$

$$\times(V\sin\beta - \dot{b}_0\cos\beta) \quad (56)$$

In the absence of underplating, the difference $\Delta\dot{W}$ is the rate at which work must be performed against gravity to move the center of mass of the fold-and-thrust belt up the decollement slope in the reference frame of the subducting plate. It is always possible to decompose the gravitational work performed on a mechanical system into the work needed to uplift the center of mass plus the work performed in the center-of-mass frame; in the present case the center-of-mass frame coincides with the reference frame of the overriding plate. It seems reasonable to assume that the steady state elevation of a fold-and-thrust belt above sea level remains constant in time. The center of mass is therefore fixed with respect to the center of mass of the Earth, and that is another reason that the first version of the mechanical energy balance is physically more appropriate.

All the integrals in equations (50) and (55) are elementary, and the resulting integrated expressions for the various rates of work are lengthy but entirely analytical:

$$\dot{W}_B = \tfrac{1}{2}\rho g\,[V + \mu_b^{-1}(1-\lambda_b)^{-1}\dot{b}_0]W(W+2x_0) \times \sin\alpha\,\sin(\alpha+\beta)\sec^2\psi_b\left[\frac{\sin 2\psi_b}{\sin 2\psi_0}\right] + \tfrac{1}{2}\rho g\,(V+\dot{b}_0\tan\psi_b)x_0^2 \times \cos\alpha\,\sin(\alpha+\beta)(\tan\psi_b - \tan\psi_0) \times \left[\frac{1+\sin\phi-\lambda\sin\phi(1+\cos 2\psi_0)}{1-\sin\phi\cos 2\psi_0}\right] \quad (57a)$$

$$\dot{W}_D = \tfrac{1}{2}\rho g W^2 \sin\alpha\,\sin(\alpha+\beta)\sec\psi_b\left[\frac{\sin 2\psi_b}{\sin 2\psi_0}\right] \times \left[Cx_0^{-1}(\cos^2\psi_b - \sin^2\psi_b)^{-1} - B(x_0+\tfrac{2}{3}W)(1-\tan^2\psi_b)\right] \quad (57b)$$

$$\dot{W}_S = \tfrac{1}{2}\rho g W\cos\alpha\,\cos\psi_0\left[\frac{2(1-\lambda)\sin\phi}{1-\sin\phi\cos 2\psi_0}\right] \times \left[C\log(1-\tan^2\psi_b) - C\log(1-\tan^2\psi_0) + 2C\tan\psi_b(\tan\psi_b - \tan\psi_0)(1-\tan^2\psi_b)^{-1} - B(\tan\psi_b - \tan\psi_0)^2(x_0^2 + x_0W + \tfrac{1}{3}W^2)\right] \quad (57c)$$

$$\dot{W}_G = \tfrac{1}{2}\rho g W(W+2x_0)(\tan\psi_b - \tan\psi_0) \times \left[U_0\sin(\alpha+\psi_0) - V_0\cos(\alpha+\psi_0)\right] + \tfrac{1}{2}\rho g WB\,(x_0^2 + x_0W + \tfrac{1}{3}W^2)(\tan\psi_b - \tan\psi_0) \times \left[2(\cos^2\psi_b - \tan\psi_0\sin\psi_b\cos\psi_b)\sin(\alpha+\psi_0) + (\tan\psi_b + \tan\psi_0 - 4\sin\psi_b\cos\psi_b)\cos(\alpha+\psi_0)\right] + \tfrac{1}{2}\rho g WC\log\left[\frac{(1+\tan\psi_b)(1-\tan\psi_0)}{(1-\tan\psi_b)(1+\tan\psi_0)}\right]\sin(\alpha+\psi_0) + \tfrac{1}{2}\rho g WC\log\left[\frac{1-\tan^2\psi_b}{1-\tan^2\psi_0}\right]\cos(\alpha+\psi_0) \quad (57d)$$

$$\dot{W}'_B = \tfrac{1}{2}\rho g\,(V+\dot{b}_0\tan\psi_b)(W+x_0)^2 \times \cos\alpha\,\sin(\alpha+\beta)(\tan\psi_b - \tan\psi_0) \times \left[\frac{1+\sin\phi-\lambda\sin\phi(1+\cos 2\psi_0)}{1-\sin\phi\cos 2\psi_0}\right] \quad (57e)$$

$$\dot{W}'_G = \tfrac{1}{2}\rho g W(W+2x_0)(\tan\psi_b - \tan\psi_0) \times \left[(U_0 - V\cos\psi_b - \dot{b}_0\sin\psi_b)\sin(\alpha+\psi_0) - (V_0 - V\sin\psi_b + \dot{b}_0\cos\psi_b)\cos(\alpha+\psi_0)\right] + \tfrac{1}{2}\rho g WB\,(x_0^2 + x_0W + \tfrac{1}{3}W^2)(\tan\psi_b - \tan\psi_0) \times \left[2(\cos^2\psi_b - \tan\psi_0\sin\psi_b\cos\psi_b)\sin(\alpha+\psi_0) + (\tan\psi_b + \tan\psi_0 - 4\sin\psi_b\cos\psi_b)\cos(\alpha+\psi_0)\right] + \tfrac{1}{2}\rho g WC\log\left[\frac{(1+\tan\psi_b)(1-\tan\psi_0)}{(1-\tan\psi_b)(1+\tan\psi_0)}\right]\sin(\alpha+\psi_0) + \tfrac{1}{2}\rho g WC\log\left[\frac{1-\tan^2\psi_b}{1-\tan^2\psi_0}\right]\cos(\alpha+\psi_0) \quad (57f)$$

We ignore underplating in all the quantitative energy balance considerations that follow.

Application to Taiwan

Using our adopted geometric and kinematic parameters and physical properties (including $\mu_b = 0.5$ and $\mu = 0.7$), we find that the rate of work performed by the subducting Eurasian plate on the Taiwan fold-and-thrust belt is

$$\dot{W}_B = 15 \text{ kW/m} \quad (58)$$

The length along strike of the region of active steady state topography in central Taiwan is about 200 km [*Suppe*, 1981], so the total power input into the steady state region is roughly 3 GW; this is approximately the amount of power supplied by three nuclear power plants, and it is about one half of the total electrical power generation of the island [*Europa Yearbook*, 1986]. If the rate of erosion is uniform, then the fractional extent to which this total work is either dissipated against decollement or internal friction or expended against gravity is

$$\dot{W}_D/\dot{W}_B = 63\% \quad (59a)$$

$$\dot{W}_S/\dot{W}_B = 22\% \quad (59b)$$

$$\dot{W}_G/\dot{W}_B = 15\% \quad (59c)$$

As expected, the form of the erosion law has a relatively small effect on the energy budget; the corresponding partition in the case of the case of linear elevation-dependent erosion is

$$\dot{W}_D/\dot{W}_B = 59\% \quad (60a)$$

$$\dot{W}_S/\dot{W}_B = 26\% \quad (60b)$$

$$\dot{W}_G/\dot{W}_B = 15\% \quad (60c)$$

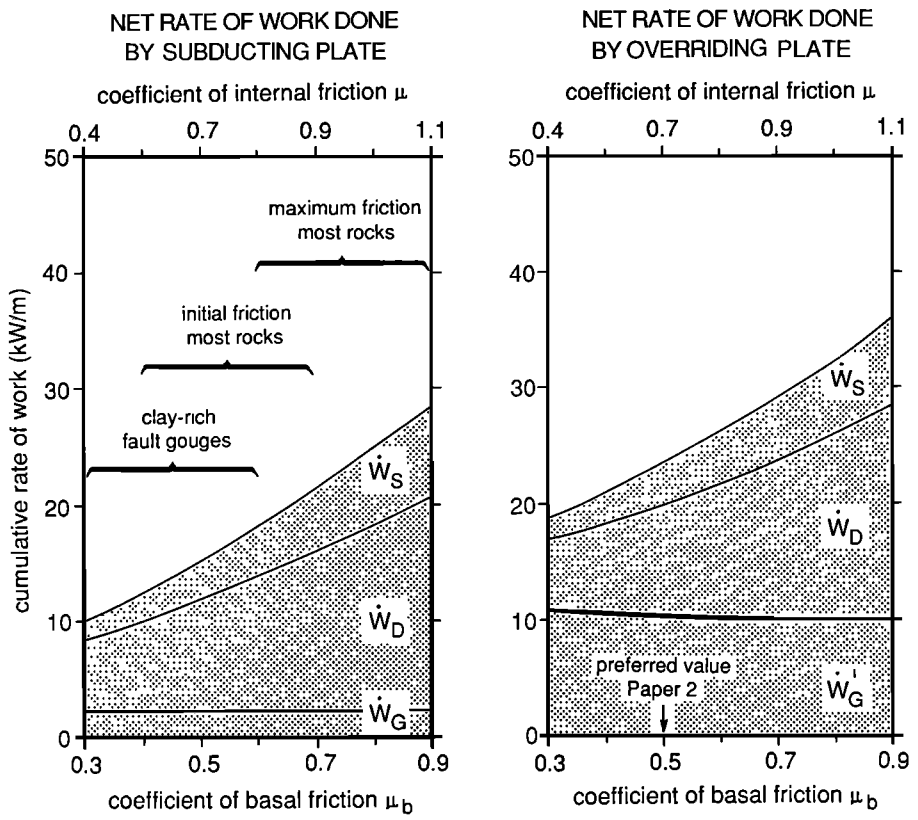

Fig. 11. Dependence of the work rates $\dot{W}_G$, $\dot{W}'_G$, $\dot{W}_D$, and $\dot{W}_S$ on the level of friction, assuming no underplating and uniform erosion $\dot{e}_0 = 5.5$ km/m.y. The coefficient of basal friction μ_b varies linearly along the bottom, and the corresponding coefficient of internal friction μ consistent with the Taiwan geometry and fluid pressure is shown along the top. (Left) The energy budget in the reference frame of the subducting plate. (Right) The energy budget in the reference frame of the overriding plate. The work rates are plotted cumulatively so that $\dot{W}_D$, for example, is given by the difference between the lowest and next lowest curve.

In either case, the amount of energy dissipated on the decollement fault is 2–3 times greater than that dissipated on the conjugate thrust faults within the wedge; elevation-dependent erosion slightly augments internal dissipation at the expense of dissipation on the decollement fault, because of the higher strain rates in the back of the fold-and-thrust belt. Regardless of the nature of the erosion law, 85% of the energy supplied by the subducting Eurasian plate is dissipated against friction, and only 15% is used to perform useful work against gravity; the total rate at which work must be done against gravity to maintain the steady state topography against erosion is 0.4 GW.

The above results describe the mechanical energy balance of the Taiwan fold-and-thrust belt from the point of view of an observer situated on the overriding Philippine Sea plate. From the viewpoint of an observer on the subducting Eurasian plate, the rate of work performed by the regional compressive stress on the back of the fold-and-thrust belt is

$$\dot{W}'_B = 23 \text{ kW/m} \tag{61}$$

The partition of this into work dissipated against decollement or internal friction or expended against gravity is

$$\dot{W}_D/\dot{W}'_B = 41\% \tag{62a}$$

$$\dot{W}_S/\dot{W}'_B = 15\% \tag{62b}$$

$$\dot{W}'_G/\dot{W}'_B = 44\% \tag{62c}$$

if the erosion rate is uniform, whereas it is

$$\dot{W}_D/\dot{W}'_B = 39\% \tag{63a}$$

$$\dot{W}_S/\dot{W}'_G = 17\% \tag{63b}$$

$$\dot{W}'_G/\dot{W}'_B = 44\% \tag{63c}$$

if the erosion rate depends linearly on the elevation. The total rate at which work is performed against gravity in the reference frame of the subducting plate is approximately 2 GW. Most of this (1.6 GW) is used to move the center of mass of the fold-and-thrust belt up the decollement slope at a rate of 70 km/m.y. Only the 0.4 GW of power expended against gravity in the center-of-mass frame is physically significant, as explained above.

The balance between the four expressions in equations (49) and (54) in all the above cases is better than 1%. As a check, we also developed analytical expressions for the neglected terms in equations (48) and (53) and verified the exact balance to machine precision.

The dependence of the various work rates on the adopted values of μ_b and μ is shown in Figure 11; the erosion is

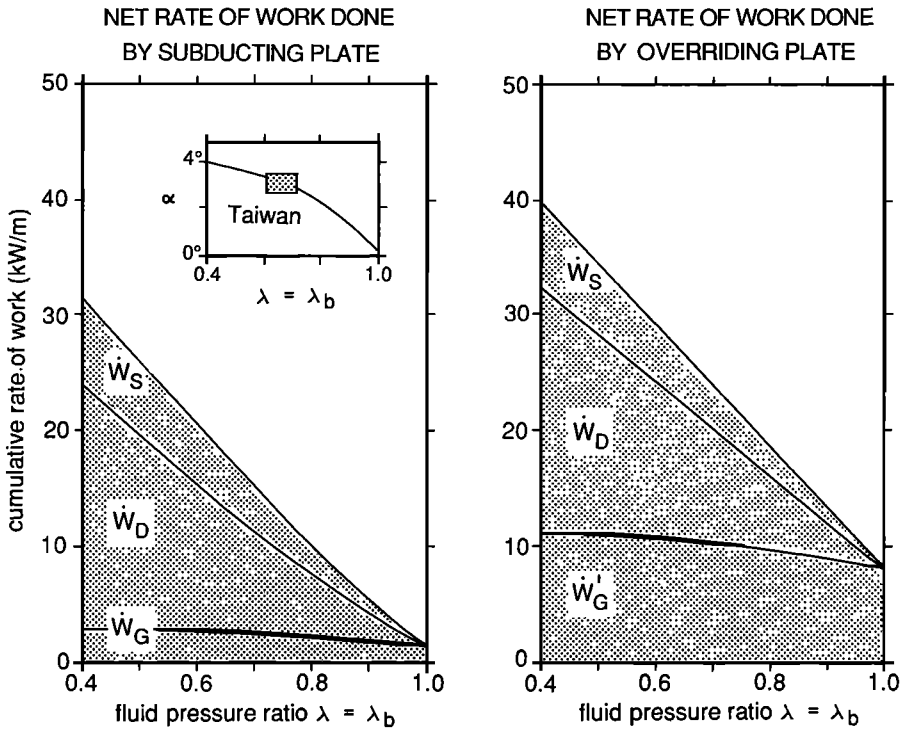

Fig. 12. Effect of the pore fluid/lithostatic pressure ratio $\lambda = \lambda_b$ on the work rates $\dot{W}_G$, $\dot{W}'_G$, $\dot{W}_D$, and $\dot{W}_S$. Inset shows the corresponding variation of the critical surface slope α; all other parameters are assumed to be those observed in Taiwan. The work rates are plotted cumulatively, as in Figure 11.

assumed to be uniform, and the work rates are plotted cumulatively, so that the highest curve on the left is the sum $\dot{W}_B = \dot{W}_G + \dot{W}_D + \dot{W}_S$, and the highest curve on the right is the sum $\dot{W}'_B = \dot{W}_D + \dot{W}_S + \dot{W}'_G$. As expected, the rate of work done against gravity in either frame is essentially independent of friction. Both $\dot{W}_D$ and $\dot{W}_S$ increase quasi-linearly with the governing coefficients of friction.

Dependence on Other Parameters

Two parameters that are known to vary widely from one fold-and-thrust belt to another, and that exert a significant control on the energy budget, are the pore fluid/lithostatic pressure ratio $\lambda = \lambda_b$ and the dip β of the basal decollement fault. To illustrate this, we consider a suite of hypothetical wedges with the same steady state width, incoming sediment thickness and accretionary influx rate as Taiwan, namely, $W = 90$ km, $l_0 = 7$ km, and $A = 500$ km^2/m.y. The inferred uniform erosion rate varies insignificantly around 5.5 km/m.y., since ψ_0 is variable and it is $\dot{e}_0 \sec\psi_0$ that is fixed by equation (31). The dependence of the cumulative work rates on $\lambda = \lambda_b$ is shown in Figure 12; both $\dot{W}_G$ and $\dot{W}'_G$ are essentially independent of the fluid pressure, but an increase in $\lambda = \lambda_b$ causes a linear decrease in $\dot{W}_D$ and $\dot{W}_S$, due to the decreased traction on the decollement and internal conjugate thrust faults. The dependence on decollement dip β is shown in Figure 13; neither $\dot{W}_D$ nor $\dot{W}_S$ depends strongly on the basal dip, nor does $\dot{W}_G$, since the upward component of velocity $\mathbf{u}$ is controlled primarily by the erosion rate. The quantity $\dot{W}'_G$, however, increases quasi-linearly with increasing β, because of the greater upward component of velocity $\mathbf{u}'$ up the decollement slope.

The effect of differing erosion rates is shown in Figure 14. Uniform erosion rates varying from $\dot{e}_0 = 5.5$ to 1.375 km/m.y. are considered; the corresponding steady state widths vary linearly along the abscissa from $W = 90$ to 360 km. The percentage work dissipated against basal friction $\dot{W}_D/\dot{W}_B$ is greater in wide, slowly eroding fold-and-thrust belts than in narrow, rapidly eroding ones such as Taiwan; both $\dot{W}_S/\dot{W}_B$ and $\dot{W}_G/\dot{W}_B$ vanish in the limit of a noneroding fold-and-thrust belt.

A twofold decrease in the uniform erosion rate $\dot{e}_0$ doubles the steady state width W, but it almost quadruples the total rate of work $\dot{W}_B$ due to the factor $W(W + x_0)$ in equation (57*a*). A twofold increase in the accretion rate A has the same effect on the steady state width W, but it causes nearly an eightfold increase in $\dot{W}_B$ because of the multiplicative factor of V in the same equation. For this reason, plate convergence velocities play a more important role than erosion rates in the mechanical energy budget of brittle frictional mountain building.

Comparison With Other Treatments

The above analysis differs significantly from the most notable previous attempt to describe the mechanical energy balance of a fold-and-thrust belt, that of *Elliott* [1976]. His reconstruction of the McConnell thrust system in the Canadian Rockies led him to support the gravity spreading hypothesis, which asserts that gravity and not a regional compressive stress is the principal force acting to emplace and deform a fold-and-thrust belt. Since he conducted his analysis in a frame of reference attached to the underlying basement, it is best compared with the second version of the mechanical energy balance described above. In the notation used here, he concluded that the quantity $\dot{W}'_G$ is negative and much greater in absolute magnitude than $\dot{W}'_B$. Our analysis shows, however, that $\dot{W}'_G$ must always be positive in any fold-and-thrust belt whose decollement dips toward its rear,

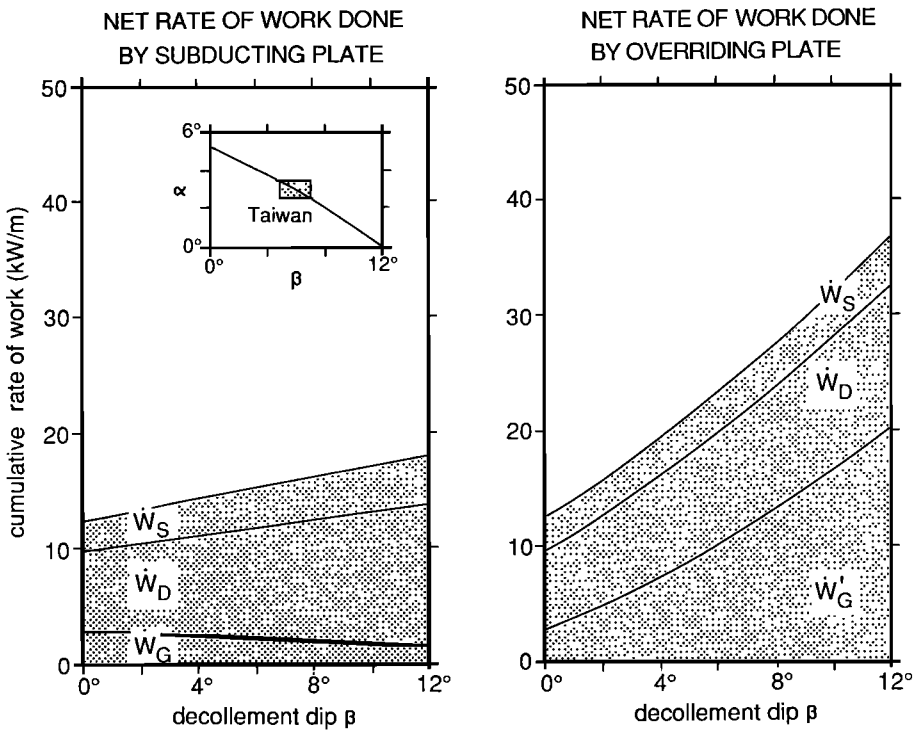

Fig. 13. Effect of the dip β of the decollement fault on the work rates $\dot{W}_G$, $\dot{W}'_G$, $\dot{W}_D$, and $\dot{W}_S$. Inset shows the corresponding variation of the critical surface slope α; all other parameters are assumed to be those observed in Taiwan. The work rates are plotted cumulatively, as in Figure 11.

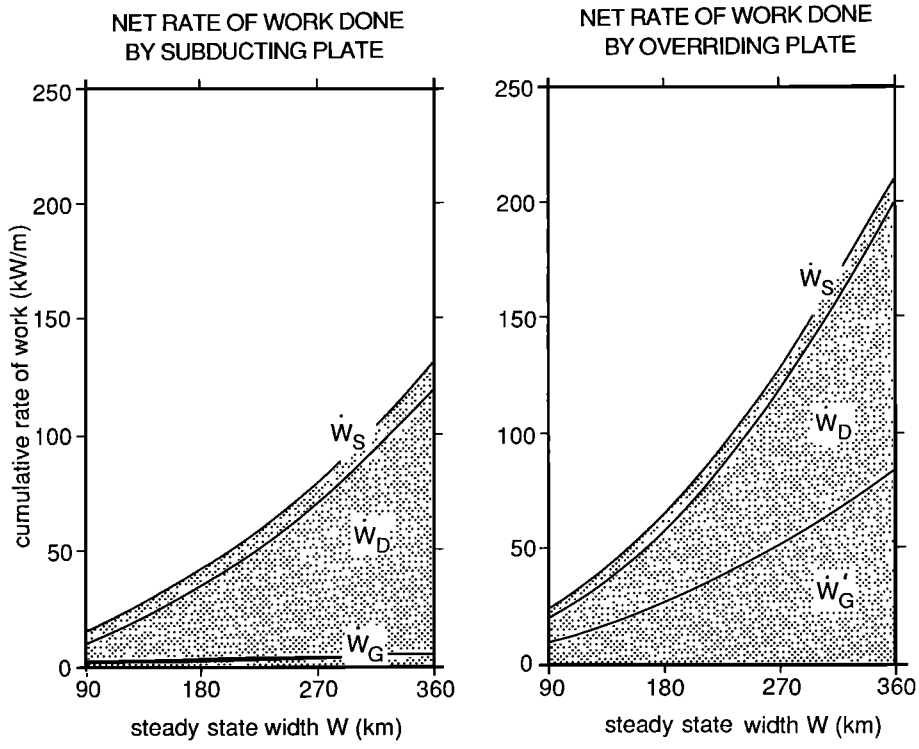

Fig. 14. Effect of the uniform erosion rate $\dot{e}_0$ on the work rates $\dot{W}_G$, $\dot{W}'_G$, $\dot{W}_D$, and W_S. The accretionary influx rate is fixed at A = 500 km^2/m.y., and the erosion rate varies from the observed high rate in Taiwan, $\dot{e}_0$ = 5.5 km/m.y., to one quarter that rate, $\dot{e}_0$ = 1.375 km/m.y. The steady state width W, which varies from W = 90 to 360 km/m.y., is used as the abscissa, and the work rates are plotted cumulatively, as in Figure 11.

because the velocity $\mathbf{u}'$ always has an upward component due to motion up the decollement, as shown in Figure 9. The rate of work performed against gravity in a reference frame attached to the basement can be negative if the basal dip β is sufficiently negative, but a decollement fault dipping toward the toe is not a geologically plausible geometry. Elliott also argued that most of the work done by gravity is dissipated within the fold-and-thrust belt rather than on its decollement fault, but our analysis shows that basal dissipation always exceeds that within the wedge for geologically reasonable values of friction and pore fluid pressure.

In a subsequent study of the Pine Mountain block in the southern Appalachians, *Wiltschko* [1979] concluded that gravity would aid the emplacement of an eroding thrust sheet, whereas it would hinder the emplacement of a noneroding one. For a steady state fold-and-thrust belt this too is contradicted by our analysis; in fact, an increase in the erosion rate $\dot{e}_0$ slightly increases $\dot{W}_G'/\dot{W}_B'$ and significantly increases $\dot{W}_G/\dot{W}_B$, as shown in Figure 14.

Two more recent analyses have considered the mechanical energy balance of common smaller-scale structural features within a fold-and-thrust belt; *Mitra and Boyer* [1986] analyzed the emplacement of a single horse in a duplex [*Boyer and Elliott*, 1982] and *Williams* [1987] analyzed the deformation of a single fault-bend fold [*Suppe*, 1983]. Qualitatively, their results are in good agreement with ours; specifically, they find that the work done against gravity in such structures is usually exceeded by the frictional dissipation on both flat and ramp faults.

Approximations Valid for a Narrow Taper

The preceding results can be simplified considerably by specializing to the case of a wedge having a narrow taper, so that $\alpha << 1$, $\beta << 1$, $\psi_0 << 1$, and $\psi_b << 1$; this should be a useful approximation for any thin-skinned fold-and-thrust belt. All the simplifications arise from the replacement of sines and tangents of small angles by the angles themselves; cosines and secants are replaced by one to the same order of approximation.

Critical Taper Model

The approximate critical taper equation takes the purely algebraic form [*Dahlen et al.*, 1984]

$$\alpha + \beta \approx \frac{\beta + \mu_b(1 - \lambda_b)}{\Lambda} \tag{64}$$

where

$$\Lambda = 1 + 2(1 - \lambda)\left[\frac{\sin\phi}{1 - \sin\phi}\right] \tag{65}$$

The shear traction on the base reduces to

$$\tau_b \approx \rho g z\,(1 - \lambda_b)\mu_b \approx \rho g z\,\alpha + \rho g z(\Lambda - 1)(\alpha + \beta) \tag{66}$$

Kinematics

We ignore underplating and consider only uniform erosion; in that case the accretion and erosion rates are related to the entering sediment thickness, subduction velocity, and distance to the deformation front by

$$\dot{A} \approx \dot{e}_0 W \approx l_0 V \approx (\alpha + \beta) x_0 V \tag{67}$$

The velocity field within the wedge reduces to

$$u \approx \left[\frac{\dot{A}(1 + x_0/W)}{\alpha + \beta}\right] x^{-1} - \left[\frac{\dot{e}_0}{\alpha + \beta}\right] \tag{68a}$$

$$v \approx \left[\frac{\dot{A}(1 + x_0/W)}{\alpha + \beta}\right] z x^{-2} - \left[\frac{\dot{e}_0}{\alpha + \beta}\right] \psi_b \tag{68b}$$

and the slip rate on the decollement fault reduces to $\Delta u \approx V - u$. A rock that enters the wedge at a point x_0, z_0 outcrops and erodes at a distance

$$x - x_0 \approx W\left[\frac{z_0/x_0 - \psi_0}{\alpha + \beta}\right] \tag{69}$$

from the deformation front; the residence time of this rock within the wedge is

$$t \approx -\dot{e}_0^{-1} W(z_0/x_0 - \psi_0) + \dot{e}_0^{-1}(\alpha + \beta)(x_0 + W) \times \log\left[\frac{\psi_b - z_0/x_0}{\alpha + \beta}\right] \tag{70}$$

These last two results are obtained by solving $dx/dt = u$ and $dz/dt = v$, using the approximate velocity field (68).

Energy Budget

The total rate of work performed on the base and front of a thin-skinned fold-and-thrust belt by the subducting plate reduces to

$$\dot{W}_B \approx \tfrac{1}{2}\rho g V\,[\Lambda H^2 - \beta(\alpha + \beta)^{-1}(H^2 - h^2)] \tag{71}$$

where $H \approx (\alpha + \beta)(x_0 + W)$ is the thickness at the back. The percentages of this total work dissipated against basal or internal friction or expended against gravity reduce to

$$\dot{W}_D/\dot{W}_B \approx (R/\Gamma)\mu_b(1 - \lambda_b) \tag{72a}$$

$$\dot{W}_S/\dot{W}_B \approx (R/\Gamma)(\Lambda - 1)(\dot{e}_0/V) \tag{72b}$$

$$\dot{W}_G/\dot{W}_B \approx 1 - R + (R/\Gamma)(\beta + \dot{e}_0/V) \tag{72c}$$

where

$$\Gamma = \beta + \mu_b(1 - \lambda_b) + \Lambda(\dot{e}_0/V) \tag{73a}$$

$$R = \frac{\mu_b(1 - \lambda_b)}{\mu_b(1 - \lambda_b) + \beta(\dot{e}_0/V)^2} \tag{73b}$$

The total rate of work performed on the back of a thin-skinned fold-and-thrust belt by the overriding plate reduces to

$$\dot{W}_B' \approx \tfrac{1}{2}\rho g V \Lambda H^2 \tag{74}$$

and its partition into the three expenditure mechanisms reduces to

$$\dot{W}_D/\dot{W}_B' \approx \mu_b(1-\lambda_b)/\Gamma \tag{75a}$$

$$\dot{W}_S/\dot{W}_B' \approx (\Lambda-1)(\dot{e}_0/V)/\Gamma \tag{75b}$$

$$\dot{W}_G'/\dot{W}_B' \approx (\beta+\dot{e}_0/V)/\Gamma \tag{75c}$$

It is noteworthy that the partition into the percentage work dissipated against basal or internal friction or expended against gravity depends only on the ratio of the erosion and subduction rates, $\dot{e}_0/V$. An alternative derivation of the above results, which employs the small-angle approximation from the outset, is given by *Dahlen* [1988] and *Barr and Dahlen* [1988].

Insensitivity to the Assumption of Isotropy

The kinematics and mechanical energy budget of a thin-skinned fold-and-thrust belt are independent of the assumption (15) that the principal strain rates and stresses are aligned. We verify that here by determining the most general form for the steady state flow of an incompressible material in an arbitrary uniformly eroding wedge. Ignoring underplating, we seek to solve

$$\frac{\partial u}{\partial x}+\frac{\partial v}{\partial z}=0 \tag{76}$$

subject to the boundary conditions

$$u\sin\psi_0 - v\cos\psi_0 = \dot{e}_0 \quad \text{on} \quad z = x\tan\psi_0 \tag{77a}$$

$$u\sin\psi_b - v\cos\psi_b = 0 \quad \text{on} \quad z = x\tan\psi_b \tag{77b}$$

and the flux balance condition

$$\dot{A} + \dot{e}_0\sec\psi_0(x-x_0) = \int_{x\tan\psi_0}^{x\tan\psi_b} u\,dz \tag{78}$$

A dimensional analysis indicates that the solution must be of the form

$$u = (\dot{A}+\dot{e}_0 x_0\sec\psi_0)x^{-1}f(\zeta) - (\dot{e}_0\sec\psi_0)g(\zeta) \tag{79a}$$

$$v = (\dot{A}+\dot{e}_0 x_0\sec\psi_0)x^{-1}j(\zeta) - (\dot{e}_0\sec\psi_0)k(\zeta) \tag{79b}$$

where f, g, j, and k are unknown functions of the similarity variable $\zeta = z/x$. Equation (76) and the basal boundary condition (77*b*) imply that

$$j = \zeta f \tag{80a}$$

$$k = \zeta g + \int_{\zeta}^{\tan\psi_b} g\,d\zeta \tag{80b}$$

The remaining boundary condition (77*a*) and the flux balance condition (78) will be satisfied provided

$$\int_{\tan\psi_0}^{\tan\psi_b} f\,d\zeta = \int_{\tan\psi_0}^{\tan\psi_b} g\,d\zeta = 1 \tag{81}$$

Collecting these results, we find that the most general form for the flow of an incompressible material in a uniformly eroding wedge is

$$u = (\dot{A}+\dot{e}_0 x_0\sec\psi_0)x^{-1}f(z/x) - (\dot{e}_0\sec\psi_0)g(z/x) \tag{82a}$$

$$v = (\dot{A}+\dot{e}_0 x_0\sec\psi_0)zx^{-2}f(z/x) - (\dot{e}_0\sec\psi_0)\left[zx^{-1}g(z/x) + \int_{z/x}^{\tan\psi_b} g(\zeta)\,d\zeta\right] \tag{82b}$$

where f and g are arbitrary, subject to the integral conditions (81).

In a narrow taper the functions f and g must be nearly constant over the small interval $\psi_0 \le \zeta \le \psi_b$. Correct to order ζ^2, we find from (81) that

$$f(\zeta) \approx g(\zeta) \approx (\alpha+\beta)^{-1} \tag{83}$$

The general solution (82) reduces to the same order to (68).

It follows that incompressibility is the principal constraint on the kinematics and mechanical energy balance of large-scale deformation in a thin-skinned fold-and-thrust belt; the assumption that the wedge material is isotropic, which is needed to obtain a unique solution in a wedge of arbitrary taper, is of minor importance.

CONCLUSIONS

About 3 GW of mechanical power are being supplied by the subducting Eurasian plate to build the rugged mountains of Taiwan and maintain them against the rapid tropical erosion. Only 0.4 GW, or 15% of this mechanical power input, is being used to perform the useful work of uplifting rocks against gravity; the remaining 85% is being frictionally dissipated, either on the basal decollement fault or internally. The resulting 2.6 GW of frictional heating have a significant effect on both the thermal structure of the fold-and-thrust belt and the pressure-temperature-time trajectories of rocks transported through it, as we show next.

Acknowledgments. This work has benefited greatly from numerous discussions with John Suppe. The frame dependence of the mechanical energy budget was pointed out to us by Norm Sleep. Financial support has been provided by the Experimental and Theoretical Geophysics Program of the U. S. National Science Foundation under grants EAR-8609991 and EAR-8804098. In addition, Terence Barr has received support from the National Science Foundation Graduate Fellowship Program.

REFERENCES

Ahnert, F., Functional relationships between denudation, relief, and uplift in large mid-latitude drainage basins, *Am. J. Sci., 268,* 243–263, 1970.

Barr, T. D., and F. A. Dahlen, Thermodynamic efficiency of brittle frictional mountain building, *Science, 242,* 749–752, 1988.

Barr, T. D., and F. A. Dahlen, Brittle frictional mountain building, 2, Thermal structure and heat budget, *J. Geophys. Res.*, this issue.

Boyer, S. E., and D. Elliott, Thrust systems, *Am Assoc. Pet. Geol. Bull., 66,* 1196–1230, 1982.

Chi, W. R., J. Namson, and J. Suppe, Stratigraphic record of plate interactions in the Coastal Range of eastern Taiwan, *Mem. Geol. Soc. China, 4,* 491–530, 1981.

Cloos, M., Flow mélanges: Numerical modeling and geologic constraints on their origin in the Franciscan subduction complex, California, *Geol Soc Am. Bull., 93,* 330–345, 1982.

Cowan, D. A., and R. M. Silling, A dynamic scaled model of accretion at trenches and its implications for the tectonic evolution of subduction complexes, *J. Geophys. Res., 83,* 5389–5396, 1978.

Dahlen, F. A., Noncohesive critical Coulomb wedges: An exact solution, *J. Geophys. Res., 89,* 10,125–10,133, 1984.

Dahlen, F. A., Mechanical energy budget of a fold-and-thrust belt, *Nature, 331,* 335–337, 1988.

Dahlen, F. A., and J. Suppe, Mechanics, growth, and erosion of mountain belts, Processes in Continental Lithospheric Deformation, edited by S. P. Clark, *Spec. Pap Geol. Soc Am., 218,* 161–178, 1988.

Dahlen, F. A., J. Suppe, and D. Davis, Mechanics of fold-and-thrust belts and accretionary wedges: Cohesive Coulomb theory, *J. Geophys Res., 89,* 10,087–10,101, 1984.

Davis, D., J. Suppe, and F. A. Dahlen, Mechanics of fold-and-thrust belts and accretionary wedges, *J. Geophys. Res., 88,* 1153–1172, 1983.

Elliott, D., The energy balance and deformation mechanisms of thrust sheets, *Philos. Trans. R. Soc London., Ser. A, 283,* 289–312, 1976.

Ernst, W. G., Mountain building and metamorphism: A case history from Taiwan, in *Mountain Building Processes,* edited by K. J. Hsü, pp. 247–256, Academic, San Diego, Calif., 1982.

Europa Yearbook, The, A World Survey, p. 744, Europa, London, 1986.

Hill, *The Mathematical Theory of Plasticity,* pp. 128–160, Clarendon, Oxford, 1950.

Hubbert, M. K., and W. W. Rubey, Role of fluid pressure in mechanics of overthrust faulting, 1, Mechanics of fluid-filled solids and its application to overthrust faulting, *Geol. Soc. Am. Bull., 70,* 115–166, 1959.

Jaeger, J. C., and N. G. W. Cook, *Fundamentals of Rock Mechanics,* pp. 87–91, Methuen, London, 1969.

Li, Y. H., Denudation of Taiwan island since the Pliocene epoch, *Geology, 4,* 105–107, 1976.

Mitra, G., and S. E. Boyer, Energy balance and deformation mechanisms of duplexes, *J. Struct. Geol., 8,* 291–304, 1986.

Peng, T. H., Y. H. Li, and F. T. Wu, Tectonic uplift rates of the Taiwan island since the early Holocene, *Mem. Geol. Soc. China, 2,* 57–69, 1977.

Pfiffner, O. A., and J. G. Ramsay, Constraints on geological strain rates: Arguments from finite strain states of naturally deformed rocks, *J. Geophys. Res., 87,* 311–321, 1982.

Ranken, B., R. K. Cardwell, and D. E. Karig, Kinematics of the Philippine Sea plate, *Tectonics, 3,* 555–575, 1984.

Rice, J. R., The mechanics of earthquake rupture, in *Physics of the Earth's Interior, Proc. Int School Phys. Enrico Fermi 78,* edited by A. M. Dziewonski and E. Boschi, pp. 555–649, North-Holland, Amsterdam, 1980.

Roecker, S. W., Y. H. Yeh, and Y. B. Tsai, Three-dimensional *P* and *S* wave velocity structures beneath Taiwan: Deep structure beneath an arc-continent collision, *J. Geophys. Res., 92,* 10,547–10,570, 1987.

Ruxton, B. P., and I. McDougall, Denudation rates in northeast Papua from potassium-argon dating of lavas, *Am. J. Sci., 265,* 545–561, 1967.

Seno, T., The instantaneous rotation vector of the Philippine Sea plate relative to the Eurasian plate, *Tectonophysics, 42,* 209–226, 1977.

Silver, E. A., M. J. Ellis, N. A. Breen, and T. H. Shipley, Comments on the growth of accretionary wedges, *Geology, 13,* 6–9, 1985.

Stallard, R. F., Weathering and erosion in the humid tropics, in *Physical and Chemical Weathering in Geochemical Cycles,* edited by A. Lerman and M. Meybeck, pp. 225–246, Kluwer Academic, Boston, Mass., 1988.

Suppe, J., Mechanics of mountain building and metamorphism in Taiwan, *Mem Geol. Soc. China, 4,* 67–89, 1981.

Suppe, J., Geometry and kinematics of fault-bend folding, *Am J Sci, 283,* 684–721, 1983.

Suppe, J., The active Taiwan mountain belt, in *The Anatomy of Mountain Ranges,* edited by J. P. Schaer and J. Rodgers, pp. 277–293, Princeton University Press, Princeton, N. J., 1987.

Wang, C. Y., and Y. L. Shi, On the thermal structure of subduction complexes: A preliminary study, *J. Geophys. Res., 89,* 7709–7718, 1984.

Williams, R. T., Energy balance for large thrust sheets and fault-bend folds, *J. Struct. Geol., 9,* 375–379, 1987.

Wiltschko, D. V., Partitioning of energy in a thrust sheet and implications concerning driving forces, *J. Geophys. Res., 84,* 6050–6058, 1979.

Wong, T. F., Shear fracture energy of Westerly Granite from post failure behavior, *J. Geophys. Res., 87,* 990–1000, 1982.

T. D. Barr and F. A. Dahlen, Department of Geological and Geophysical Sciences, Princeton University, Guyot Hall, Princeton, NJ 08544.

(Received April 28, 1988;
revised December 16, 1988;
accepted October 12, 1988.)